The 2016 landslide at Saint-Luc-de-Vincennes

Tremblay-Auger, F., Locat, A. & Leroueil, S.
Département de génie civil et de génie des eaux – Université Laval, Québec, Québec, Canada
Locat, P., Therrien, J., Demers, D., Mompin, R.
Ministère des Transports, Mobilité Durable et Électrification des Transports, Québec, Québec, Canada

ABSTRACT
The Saint-Luc-de-Vincennes landslide occurred on November 9th 2016, 100 km west of Quebec City, Canada, in a sensitive marine clay terrace. The particularity of this event is that there are evidences that the movement started as a flow and finished as a spread. The final morphology shows horsts and grabens typical of spread and also a large quantity of remolded material that flowed out of a bottleneck shaped crater, which is typical of flowslides. The geotechnical investigation of this landslide was performed by the Ministère des Transports, de la Mobilité Durable et de l'Électrification des Transports (MTMDET) in collaboration with Université Laval. Several studies were used to determine the location of the failure surface and also to acquire information on the properties of the clay deposit. It was also possible to reconstitute the different phases and the chronology of this particular landslide. The geotechnical characterization and morphological analysis of this unique landslide give new insights on the kinematic of large landslides in sensitive clays.

RÉSUMÉ
Un glissement a eu lieu le 9 novembre 2016 près de la municipalité de Saint-Luc-de-Vincennes, à 100 km à l'ouest de la ville de Québec, au Canada. Ce dernier s'est produit dans une terrasse d'argile marine sensible et présente la particularité d'avoir débuté par une coulée argileuse et de s'être terminé par un étalement. La morphologie finale présente des horsts et des grabens typiques des étalements, ainsi qu'une grande quantité de matériel remanié s'étant écoulé hors d'un cratère en forme en goulot, caractéristique des coulées argileuses. L'investigation géotechnique de ce glissement a été entreprise par le Ministère des Transports, de la Mobilité Durable et de l'Électrification des Transports (MTMDET) en collaboration avec l'Université Laval. Les différents sondages ont permis de localiser la surface de rupture et de décrire les propriétés géotechniques de l'argile en place. Il a également été possible de faire une analyse morphologique du glissement, ainsi que de déterminer la séquence des évènements, permettant d'apporter de nouvelles connaissances sur la cinématique des grands glissements de terrain dans les argiles sensibles.

1 INTRODUCTION

The post-glacial marine sensitive clays in Québec are very prone to large retrogressive landslides, which occur generally along watercourse banks (Demers et al. 2017). Demers et al. (2014) and Locat et al. (2017) recognize two major types of retrogressive landslide; "flowslide" and "spread", involving two different failure mechanisms and presenting typical debris and scar morphologies. The typical width of spreads is generally larger than the retrogression distance, and their opening along the river is generally wide. The alternation of horsts and grabens gives to their scars a specific morphology, called "thump-print" by Mollard and Hughes (1973). In the cases of flowslides, the scars may present various morphologies, because the multiple successive failure mechanism can evolve in many directions. However, the "pear-shaped" depression, with a small "bottleneck" near the initial slope, was considered for a long time as a typical flowslide scar (Chagnon 1968; Karrow 1972), because it was supposed that material must be much remolded to pass over a small opening to the watercourse.

The Saint-Luc-de-Vincennes landslide occurred on November 9th 2016 in a sensitive marine clay terrace, near the Champlain River, 100 km west of Quebec City, in Canada (see localization on figure 1). The crater of the landslide is approximately 160 m wide and 177 m long. This case is very interesting because the final morphology shows horsts and grabens typical of spread and also a large quantity of remolded material that flowed out of a pear-shaped crater, with a small bottleneck (see figure 2), which is typical of flowslides. Moreover, some observations were made by the landowner on the sequence of the movement and lidar data and aerial photos are available before and just after the events.

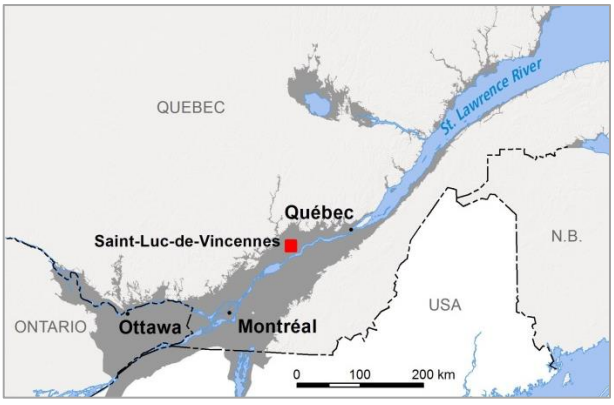

Figure 1. General localization of the site

As a result of the originality of this movement, a complete morphological study of the debris was made to establish the sequence of the events and to delimit the part of the land involved in the flow and the one associated with the spread. This paper presents the field observations and investigation, the geotechnical characterization of the site, the morphological analysis of the landslide, including the reconstitution of the initial slope and volume calculations, and a discussion on the sequence of the events and the differences between flowslides and spreads.

2 DESCRIPTION OF THE EVENT

The landslide occurred along a broad meander of the Champlain River, where the initial height of the bank is 18 m. On October 22nd, the landowner observed what seemed to be small rotational slides near the toe of the riverbank. Then some days later, followed a larger one involving the entire slope and reaching the fence placed just at the edge of the slope. These failures slightly expanded in the following days until a first episode of flow that occurred around November 7th (date where the landowner took the first pictures of the landslide). By this time, the scar had reached the plateau at the top of the slope and was already at a distance of about 56 m from the edge of the initial slope. Contacted by the landowner, an employee from the Ministère de la Sécurité Publique du Québec (MSP) visited the field and took pictures of this first flowslide on November 9th (see figure 3). About 23h30 on the evening of the same day, the landowner heard ground noises and felt vibrations for a short period of time. He went out and saw the major landslide scar (visible on figure 2). The resulting scar stays approximately the same after this moment, with just little subsidence around the backscarp and some minor rotational failures the day after, around higher lateral scarp near the bottleneck (see figure 2).

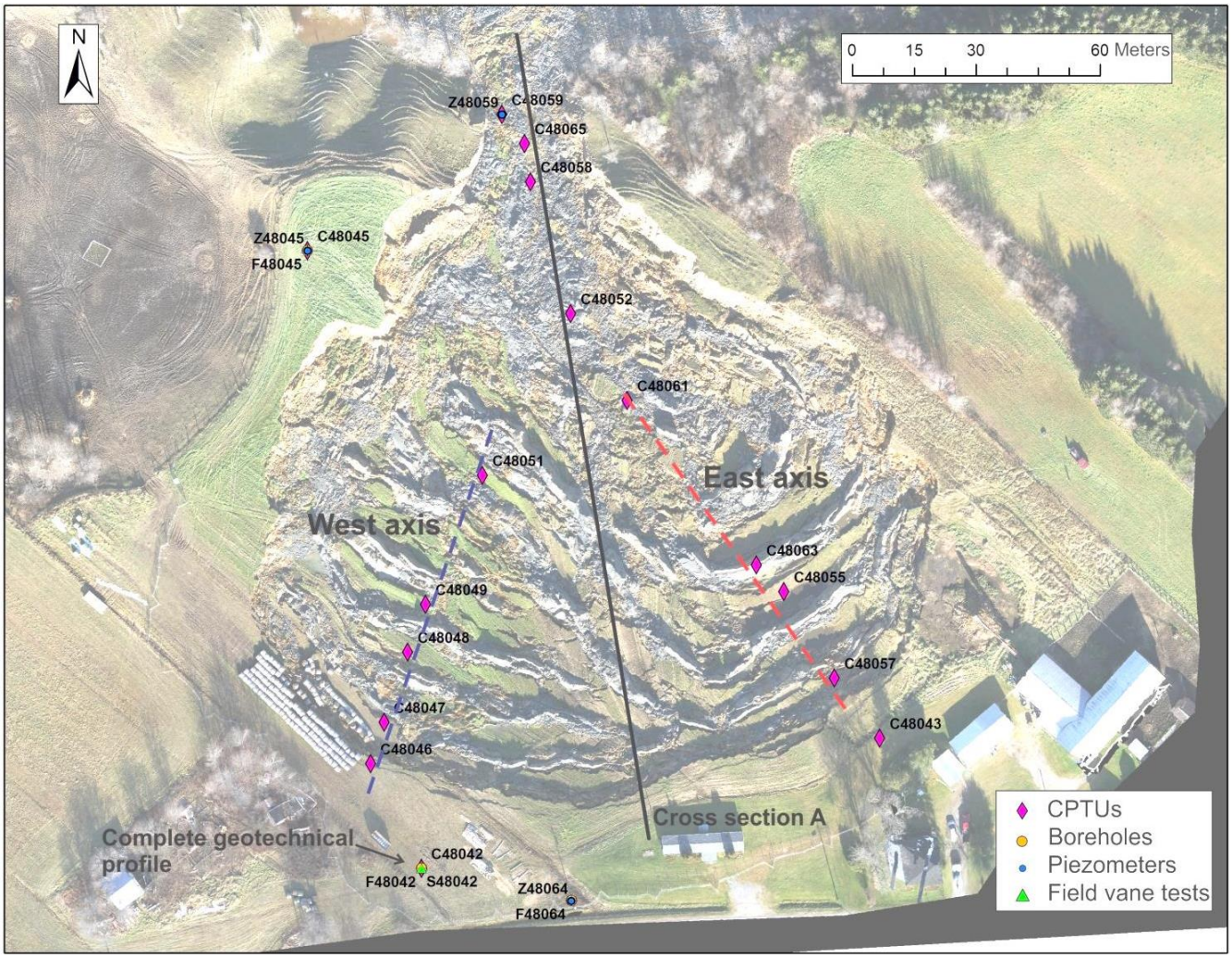

Figure 2. Localization of the geotechnical studies, the cross section A is shown in black, the west axis in blue, east axis in red and the complete geotechnical profile at location 48042 (aerial photograph taken after the event)

Figure 3. View of the scar of the first episode of flowslide, taken on November 9th 2016, a few hours before the major event

3 FIELD AND LABORATORY INVESTIGATION

The geotechnical investigation of the site was carried out by the MTMDET in collaboration with Université Laval, from December 2016 until March 2017. During this period, a total of 15 piezocone tests with pore pressure measurements (CPTUs), 3 boreholes and 1 field vane test were performed. Piezometer nests were installed at 3 spots on the site (see location on figure 2). An aerial lidar survey was already available (2011) and a new one was done three days after the event to obtain the final morphology of the debris. Vertical and oblique aerial photographs of the landslide were also taken at the same time. Laboratory tests were carried out on samples from location 48042 (figure 2) including oedometer tests, grain-size distribution, water content (w), consistency limits (plastic limit, w_p, and liquid limit, w_l) and sensitivity (St) calculated from the intact (Su) and remolded (Su_r) shear strengths from the Swedish fall cone.

4 GEOTECHNICAL CHARACTERIZATION

With the information acquired during the geotechnical investigation, it was possible to generate a complete geotechnical profile at the location 48042 (see figure 2) and a cross section showing ground surface elevations before and after the event as well as the elevation of the failure surface (see cross section A on figure 2).

4.1 Geotechnical properties of the site

The complete geotechnical profile at the location 48042 is presented on figure 4. A homogeneous silty clay deposit with traces of sand can be identified. The percentage of clay particles varies between 44 and 67 %, silt particles between 33 and 56 % and sand particles between 0 and 1.4 %. A very thick clay deposit starts at a depth of 2 m, right under a crust layer, to depth greater than 100 m, according to previous geophysical soundings around the site. The CPTUs carried on at the site were voluntarily stopped at a depth of 50 m, so the real thickness of the clay layer is unknown. Samples were taken every 2 m up to a depth of 24 m, approximately 6 m under the river level.

The CPTU's corrected tip resistance (q_t) increases with depth from 300 to 1900 kPa between 2 and 50 m of depth. The water content decreases with values from 95% to 53% between 2 and 24 m. The liquidity index (I_L) shows values higher than unity, confirming that the clay is sensitive, and it tends to decrease throughout the layer from 1.79 to 1.02. The plasticity index (I_P) is varying between 40 and 27 and also tends to decrease with depth. The undrained shear strength obtained from the field vane tests (Su) indicates a firm to stiff clay deposit with values from 20 kPa at a depth of 2 m to 60 kPa at a depth of 24 m. A N_{kt} of 14 was obtained to correlate the undrained shear strength obtained from the field vane test to the corrected tip resistance (q_t), which is a normal value for eastern Canadian clay (Leroueil 1997). The clay deposit is overconsolidated with values of OCR varying between 3.9 and 1.6 up to a depth of 29 m. Under this depth, the OCR values are around 1.1, showing that the deposit is slightly overconsolidated.

The pore pressures from piezometer 48064, represented by the blue cross on figure 4, show values slightly lower than hydrostatic conditions, indicating the presence of a downward gradient at this location.

4.2 Topography and localization of the failure surface

The failure surface was located with the CPTUs performed inside the landslide area; there is an observable distinction in the corrected tip resistance (q_t) and pore pressures (u) profiles in the debris versus those in the intact material. It can be observed on figure 2 that the CPTUs were done along two main axes.

On figure 5, the elevation of the failure surface along those two axes was compared. CPTUs from the east axis are presented in red, those from the west axis in blue and those from the central axis in black. The initial topography of the slope before the event is shown by a dashed line and the final topography by a full line. It can be observed that the elevation of the failure surface is almost identical along the two axes and close to the horizontal between a distance of 45 and 110 m. The elevation of the failure surface then slightly decreases after a distance of 110 m. The abrupt rise of the elevation observed for the sounding C48065, around a distance of 168 m, is possibly due to an error during the elevation survey.

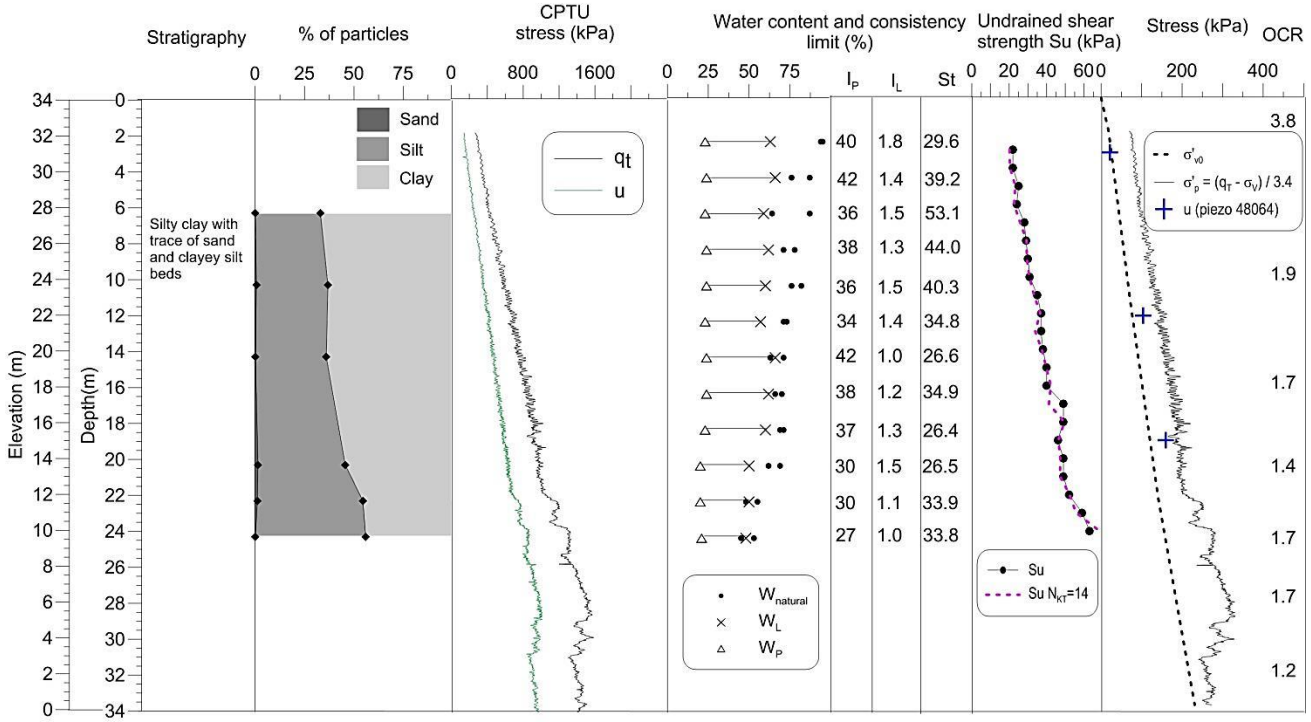

Figure 4. Complete geotechnical profile at location 48042

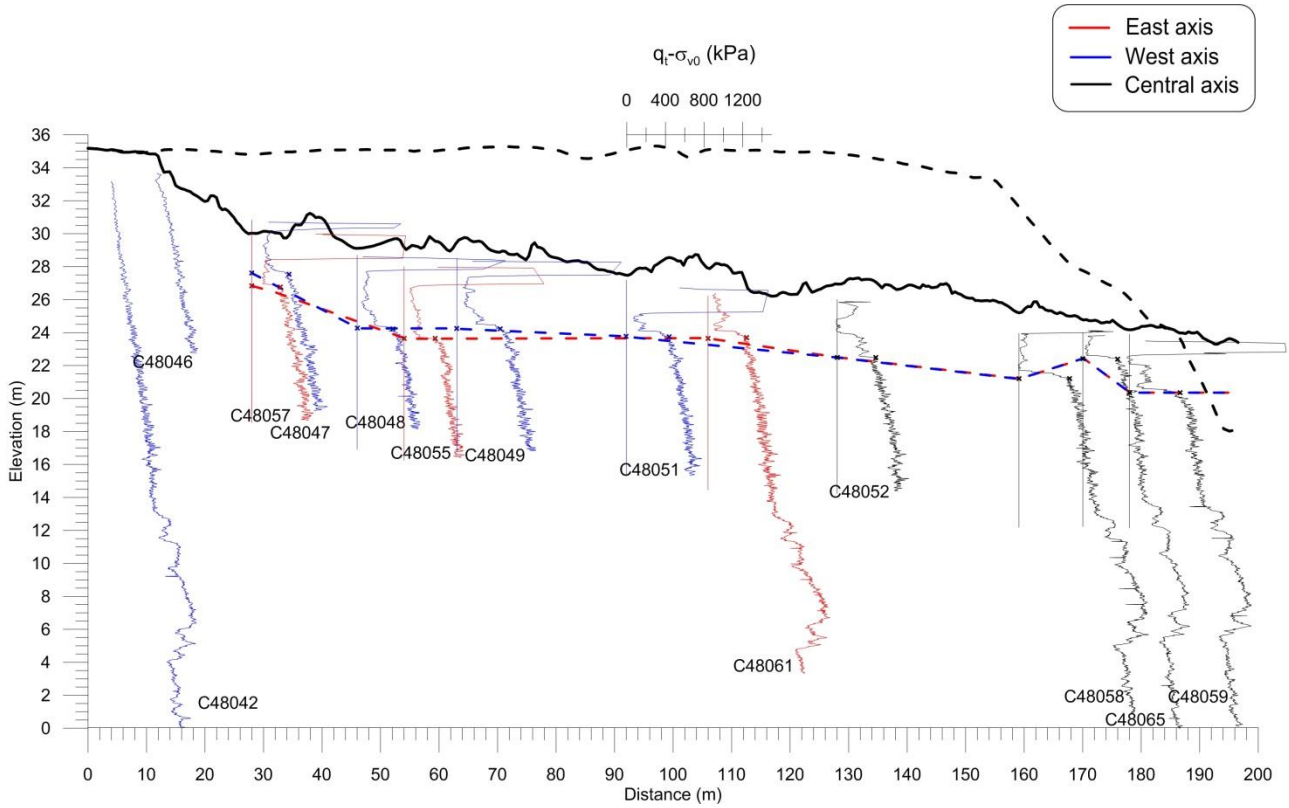

Figure 5. Cross section A showing the comparison of the elevation of the failure surface along the east axis in red and the west axis in bleu (Initial topography is depicted by a black dashed line and the final topography by a full black line)

5 MORPHOLOGICAL ANALYSIS OF THE LANDSLIDE

Field observations and photos taken by the landowner and the MSP the days and hours before the major event showed evidence of a first episode of flow. From the field observations made after the event and on lidar and aerial photographs, a bottleneck shaped crater was formed and a high quantity of remolded material flows out in the river on a distance of 680 m. Many hay bales, standing originally in the middle of the field (see figure 6) were also transported several tens of meters away in the Champlain River, with the rest of the remoulding material. This first episode of movement probably occurred in the evening, some hours after the visit of the employee of the MSP.

Horsts and grabens, beginning at the end of the landslide scar and trapped in the crater, were also identified (see figure 2). This evidence shows that a spread occurred shortly after the flowslide and was the last episode of movement, probably the one heard by the landowner. The change in the failure surface elevation on figure 5, which is explained in Section 4.2 and occurred at a distance of 110 m, could distinguish those two zones. In accordance with this hypothesis, a reconstitution of the initial slope with the grabens, coupled with some volume calculations, allows to delimit the land implicated in the flowslide and the one involved in the spread.

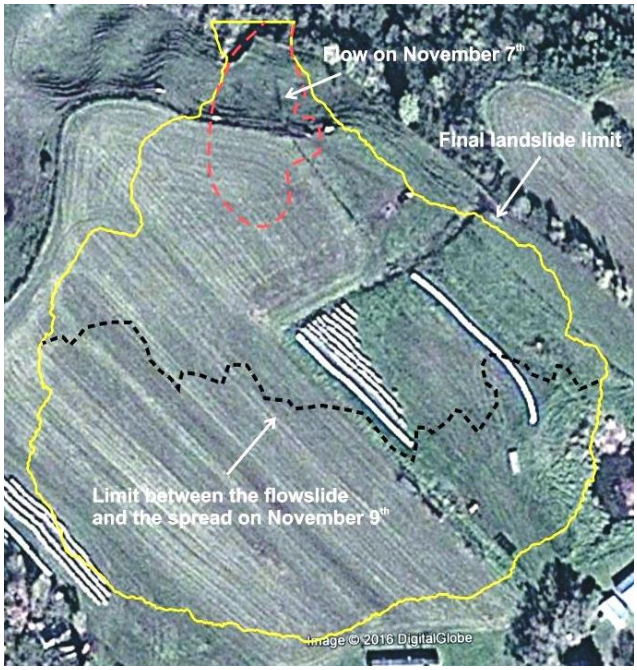

Figure 6. Delineation of the first episode of flow on November 7th in red dashed line and the limit between the flowslide and the spread of the main event on November 9th in black dashed line (aerial photograph taken from Google Earth - 2016)

5.1 Reconstitution of the initial field

For the reconstitution of the initial field, two methods were used. The first one used the mosaic of the vertical aerial photographs taken after the event. On this picture, the grabens were delimited with a photo-processing software and extracted separately as objects (see figure 7). Afterward, with ArcGIS software, the grabens were approximately placed manually to their original position using the georeferencing tool. Visual clues like lines in the field, location of pits and the vegetation helped to reassemble the puzzle.

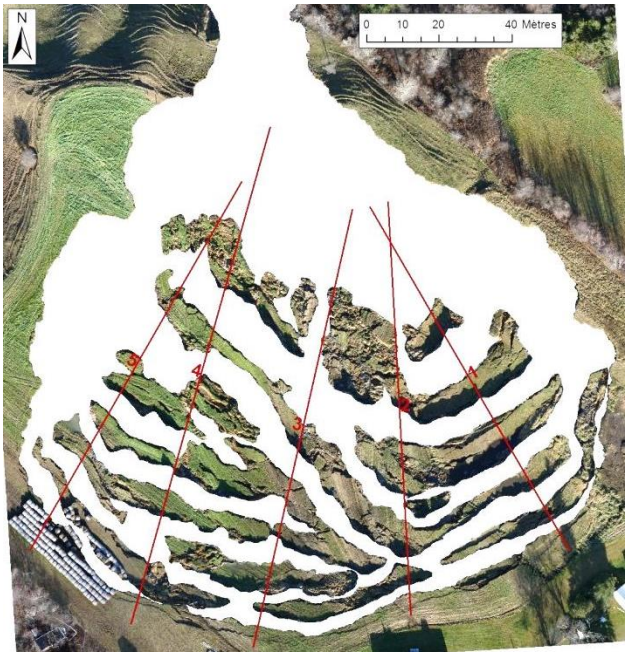

Figure 7. Delimitation of the grabens and the location of the 5 cross sections

The second method used 5 cross sections traced parallel to the flow direction of the debris (see figure 7). The initial and final topography along those axes were extracted from the lidar's data. The grabens and the horsts were placed as closely as possible along those cross sections to their initial location. Figure 8 shows an example for the fourth cross section. The failure surface is depicted in purple dashed line, the initial topography in black dashed line and the grabens are in green. Part a) shows the final location of the grabens and part b) the approximate relocation of those grabens and horsts along the initial topography. The limit of the spread is also shown in part b); it is at the position of 66 m in this case.

The 5 cross sections gave 5 limits for the spread that were then compared to the aerial reconstitution. Figure 9 shows the final reconstitution; the black dashed line depicted the limit of spread obtained from the aerial reconstitution and the 5 yellow stars represent the limit of spread obtained from each cross section. For the first and second cross sections the limits fit perfectly. For the three others, there is a difference of several meters. This can be explained by the fact that reconstitution with the cross sections does not take into account that some grabens were deformed and reoriented during the spread. Hence, the initial and final emplacement of those grabens may not

be on the same line. Overall, the two approaches give essentially the same results, showing that approximately half of the land was affected by the spread, and the other half by the flow.

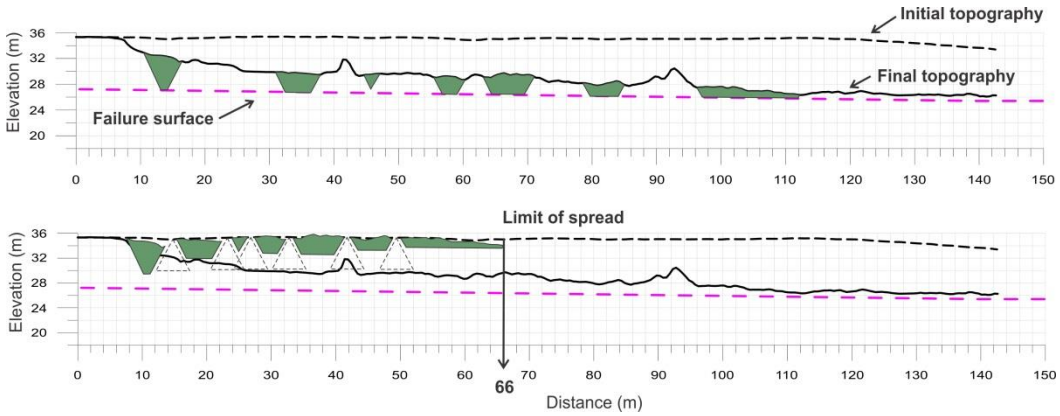

Figure 8. Cross section 4; part a) Final position of the grabens along the final topography, part b) Estimated initial location of the grabens and the horsts along the initial topography

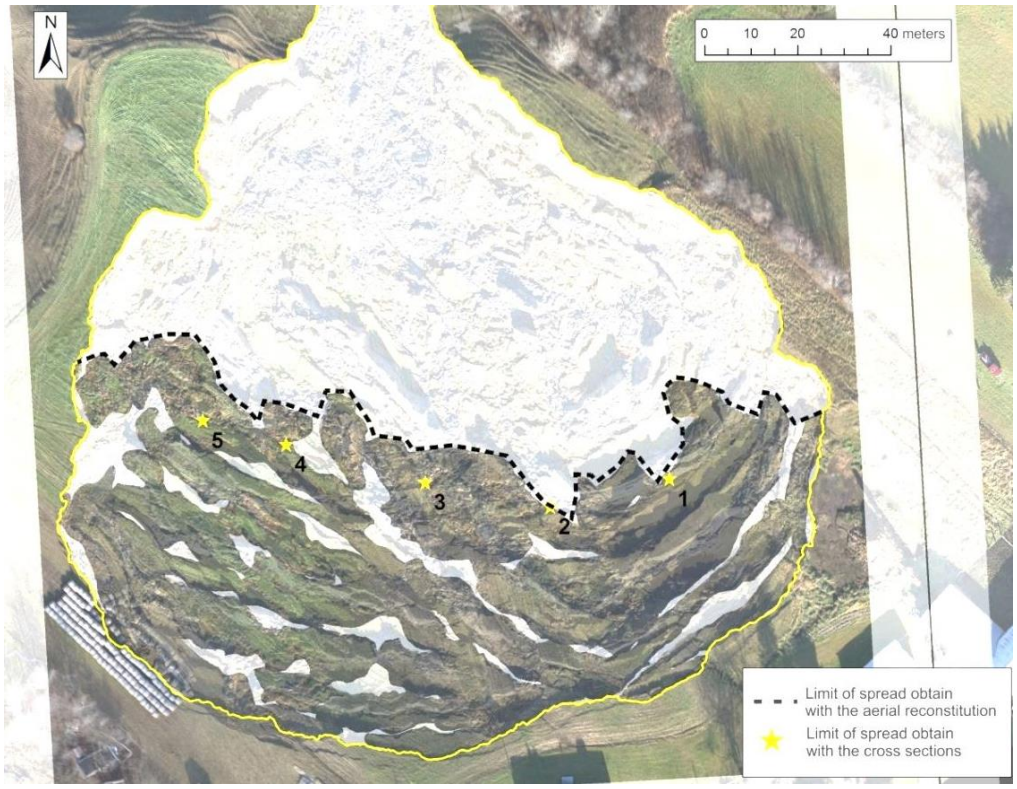

Figure 9. Final reconstitution of the land involved in the spread showing the two methods; aerial reconstitution and cross section reconstitution (aerial photograph taken after the event)

5.2 Volumes calculations

With the lidar surveys performed before and after the event, different volumes were calculated to estimate the soil mass involved in the flowslide and in the spread. From the previous analysis, all the debris from the flowslide exited the crater, while all the debris from the spread (horsts and grabens) remained trapped. Figure 10 shows a sketch of the volume calculations. The limit obtained from the reconstitution described in section 5.1 was used to calculate the volumes presented in table 1.

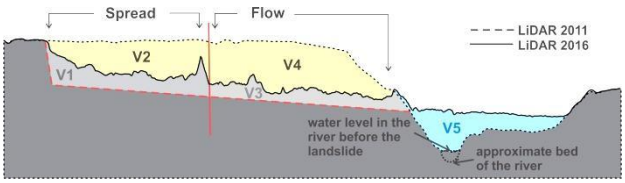

Figure 10. Sketch of the different volumes calculated

Table 1. Different volumes calculated

Area	Volume (m^3)
V1	53 223
V2	45 639
V3	43 541
V4	54 796
V5	69 324

With this assumption, the portion of the intact land involved in the spread refers to V1 plus V2 and appears to be equivalent to the volume of the debris remaining in the crater, i.e. V1 plus V3. Those two volumes are similar with values of respectively of 98 862 m^3 and 96 764 m^3, confirming that the limit is nearly exact. Also, the portion of the land involved in the flowslide refers to V3 plus V4 (98 337 m^3) and should be equivalent to the volume of the debris, which refers to V2 plus V4 (100 435 m^3). Since all the debris went out of the carter, the volume V5 (69 324 m^3) of debris in the river would also belong to the flowslide debris and should be equivalent to the two other volumes. The first volumes are effectively similar, but the value of V5 is quite smaller than the other values that are around 100 000 m^3.

The difference between this value and the two others is possibly due to the quantity of debris under the water surface of the river, which is not taken into account in the analysis. Effectively, because lidar surveys cannot penetrate water, the topography given by the 2011 lidar (before the event) shows the water level in the river at this moment. However, a major quantity of debris could have deposited at the bottom of the river, and then be neglected in the calculation of the volumes. It is known that the thickness of water in the river is approximately 1 m. Also, the debris from the flowslide progressed on a distance of roughly 680 m (up and down the river) and the river is about 15 m wide. With this ascertainment, a volume of 10 200 m^3 of debris can be added to the previous volume V5, giving a value of 79 524 m^3. This value is closer to the one expected of 100 000 m^3, but the calculation for the volume of debris in the water is approximate. The rest of the volume is probably under the water that flooded the upstream part of the river.

6 DISCUSSION

6.1 Sequence of the events

With the first pictures taken by the landowner on November 7th, it was possible to delimit approximately the first flow that took place on that date (see red dashed line on figure 6). On November 9th, the MSP took some pictures, and except for some small blocks of soil, no extension of the flow scarp was noticed (see figure 3). The latter is roughly 37 m wide and 56 m long.

At about 23h30 on November 9th, the landowner was awakened by a big noise and observed the complete failure of his land. As described in section 5, this major event could be separated in two different types of landslide: flow and spread. The black dashed line on figure 6 shows the separation between those two episodes. It is assumed that the two events took place in a short period of time, as the landowner did not perceive two different landslides. It is important to point out that the orientation of the study toward a two-event landslide was not confirmed by any visual witnesses.

6.2 Particularities of flowslides and spreads

Up to now, large retrogressive landslides as flowslides and spreads apparently occurred independently and have been studied separately. Flowslides result from a succession of rapid rotational failures that generally occur rapidly under undrained conditions. During the process, part of the material is remolded and becomes very fluid, so the debris tend to flow out and leave an essentially empty crater. As previously mentioned, pear-shaped scars are considered typical with this failure mechanism. The characteristics of the first phase of the 2016 event are consistent with this description.

Otherwise, in spreads, there are formation of horsts and grabens of intact material overlying a shear zone of remolded material (Locat et al. 2011). Unlike flowslides, the debris can stay in the crater or flow a little bit out (Demers et al. 2014). This has been possible at Saint-Luc-de-Vincennes because the flow gave room for spreading. As a result, the Saint-Luc-de-Vincennes landslide shows a mixed morphology of those two kinds of landslide. Such a situation was rarely observed, but fragmentary information shows a similar phenomenon in the cases of St-Thuribe 1898 (Dawson, 1899), St-Prosper 1953 (Karrow, 1972), Lemieux 1993 (Locat et al, 2015) and Mink 1993 (Geertsema, 2006).

As bottleneck shaped crater can only allow the remolded debris to flow out, the flowslide would have left an unstable back scarp giving the appropriate conditions for a spread to be initiated and to propagate up to the observed final back scarp of the landslide.

7 CONCLUSION

The Saint-Luc-de-Vincennes landslide that occurred on November 9th 2016 is the first one of a composite movement “flowslide/spread” to have been well documented and analyzed by the MTMDET and Université Laval. This particular landslide started with several rotational slides around October 22nd, then a first episode of flowslide occurred on November 7th and finally, the major event that combined a flowslide and then a spread followed the same day, a few hours later. After the field investigation, it was possible to characterize the clay deposit and to establish the elevation of the failure surface. A morphological analysis of the debris of the landslide was

then done to reconstitute the initial slope before the spread. This analysis coupled to some volume calculations allowed to establish the limit between the flowslide and the spread. The sequence of the events was then described with more certainties and was confirmed by the known characteristics of those two kinds of landslide. The study of this unique landslide gave new insights on the kinematic of large landslides and strengthens the ones already acquired in sensitive clays.

8 ACKNOWLEDGMENT

The authors would like to acknowledge the MTMDET for the permission for using their data, and the Plan d'action 2013-2020 sur les changements climatiques and the Fond Vert 2013-2020 for their financial contribution of 333 882,50$. The Natural Sciences and Engineering Research Council of Canada is also recognized for its financial support.

9 REFERENCES

Chagnon J.Y. 1968. Les coulées d'argile dans la province de Québec. Naturaliste can., 95, 1327-1343.

Dawson G.M. 1899. Remarquable landslid in Portneuf County, Québec. Geological Survey of America,10, 483-490.

Demers, D., Robitaille, D., Locat, P., Potvin, J. 2014. Inventory of Large Landslide in Sensitive Clay in the Province of Québec, Canada : Preliminary Analysis, *Landslides in Sensitive Clay : From Geosciences to Risk Management,* L'Heureux et al. eds. Springer, p.77-89.

Demers, D., Robitaille, D., Lavoie, A., Paradis, S., Fortin, A., Ouellet, D., 2017. The use of Lidar airborne data for retrogressive landslides inventory in sensitive clays, Québec, Canada. In: Thakur, V., L'Heureux, J.S., Locat, A. (Eds.), Landslides in Sensitive Clays: From Research to Implementation. Springer, Netherlands, pp. 279–288.

Geertsema, M., Cruden, D.M., Schwab, J.W., 2006. A large, rapid landslide in sensitive glaciomarine sediments at Mink Creek, northwestern British Columbia, Canada. Engineering Geology 83, 36–63.

Karrow P.F. 1972. Earthflows in the Grondines and the Trois-Rivières Areas, Québec. Can. Journ. Of Earth Sciences, 9, 561-573.

Leroueil S. 1997. Geotechnical characteristics of eastern Canada clays, *Workshop on soft clays,* Yokosuka, Japan.

Locat, A., Leroueil, S., Bernander, S., Demers, D., Jostad, H.P., and Ouehb, L. 2011. Progressive failures in eastern Canadian and Scandinavian sensitive clays. *Canadian Geotechnical Journal*, 48(11): 1696–1712.

Locat P., Demers D., Locat A., Leroueil S., 2015. Investigations complémentaires du glissement de terrain de Lemieux de 1993 sur la rivière Nation Sud, à Lemieux, Ontario. Can. Geotech. Conf. proceedings.

Mollard J.D. & Hughes G.T., 1973. Earthflows in the Grondines and the Trois-Rivières Areas, Québec: Discussion. Can. Journ. Of Earth Sciences, 10, 324-326.